





## Article

# Developing Robust Flood Susceptibility Model with Small Numbers of Parameters in Highly Fertile Regions of Northwest Bangladesh for Sustainable Flood and Agriculture Management

Showmitra Kumar Sarkar <sup>1</sup>, Saifullah Bin Ansar <sup>1</sup>, Khondaker Mohammed Mohiuddin Ekram <sup>1</sup> , Mehedi Hasan Khan <sup>1</sup> , Swapan Talukdar <sup>2</sup> , Mohd Waseem Naikoo <sup>2</sup> , Abu Reza Towfiqul Islam <sup>3</sup>, Atiqur Rahman <sup>2,\*</sup> and Amir Mosavi <sup>4,5,6</sup>

<sup>1</sup> Department of Urban and Regional Planning, Khulna University of Engineering and Technology (KUET), Khulna 9203, Bangladesh; mail4dhrubo@gmail.com (S.K.S.); kuetsiam30@gmail.com (S.B.A.); mohiuddinekram@gmail.com (K.M.M.E.); plannermehedi@gmail.com (M.H.K.)

<sup>2</sup> Department of Geography, Faculty of Natural Science, Jamia Millia Islamia, New Delhi 110025, India; swapantalukdar65@gmail.com or pdf.stalukdar@jmi.ac.in (S.T.); waseemnaik750@gmail.com (M.W.N.)

<sup>3</sup> Department of Disaster Management, Begum Rokeya University, Rangpur 5400, Bangladesh; towfiq\_dm@brur.ac.bd

<sup>4</sup> John von Neumann Faculty of Informatics, Obuda University, 1034 Budapest, Hungary; mosavi.amirhosein@uni-nke.hu

<sup>5</sup> Institute of Information Engineering, Automation and Mathematics, Slovak University of Technology in Bratislava, 81237 Bratislava, Slovakia

<sup>6</sup> Institute of Information Society, University of Public Service, 1083 Budapest, Hungary

\* Correspondence: arahman2@jmi.ac.in



**Citation:** Sarkar, S.K.; Ansar, S.B.; Ekram, K.M.M.; Khan, M.H.; Talukdar, S.; Naikoo, M.W.; Islam, A.R.T.; Rahman, A.; Mosavi, A. Developing Robust Flood Susceptibility Model with Small Numbers of Parameters in Highly Fertile Regions of Northwest Bangladesh for Sustainable Flood and Agriculture Management. *Sustainability* **2022**, *14*, 3982. <https://doi.org/10.3390/su14073982>

Academic Editor: Jurgita Antuchevičienė

Received: 12 February 2022

Accepted: 20 March 2022

Published: 28 March 2022

**Publisher's Note:** MDPI stays neutral with regard to jurisdictional claims in published maps and institutional affiliations.



**Copyright:** © 2022 by the authors. Licensee MDPI, Basel, Switzerland. This article is an open access article distributed under the terms and conditions of the Creative Commons Attribution (CC BY) license (<https://creativecommons.org/licenses/by/4.0/>).

**Abstract:** The present study intends to improve the robustness of a flood susceptibility (FS) model with a small number of parameters in data-scarce areas, such as northwest Bangladesh, by employing machine learning-based sensitivity analysis and an analytical hierarchy process (AHP). In this study, the nine most relevant flood elements (such as distance from the river, rainfall, and drainage density) were chosen as flood conditioning variables for modeling. The FS model was produced using AHP technique. We used an empirical and binormal receiver operating characteristic (ROC) curves for validating the models. We performed Sensitivity analyses using a random forest (RF)-based mean Gini decline (MGD), mean decrease accuracy (MDA), and information gain ratio to find out the sensitive flood conditioning variables. After performing sensitivity analysis, the least sensitivity variables were eliminated. We re-ran the model with the rest of the parameters to enhance the model's performance. Based on previous studies and the AHP weighting approach, the general soil type, rainfall, distance from river/canal (Dr), and land use/land cover (LULC) had higher factor weights of 0.22, 0.21, 0.19, and 0.15, respectively. The FS model without sensitivity and with sensitivity performed well in the present study. According to the RF-based sensitivity and information gain ratio, the most sensitive factors were rainfall, soil type, slope, and elevation, while curvature and drainage density were less sensitive parameters, which were excluded in re-running the FS model with just vital parameters. Using empirical and binormal ROC curves, the new FS model yields higher AUCs of 0.835 and 0.822, respectively. It is discovered that the predicted model's robustness may be maintained or increased by removing less relevant factors. This study will aid decision-makers in developing flood management plans for the examined region.

**Keywords:** flood susceptibility; remote sensing; MCDM; machine learning; sensitivity; natural hazards; artificial intelligence; extreme events; big data; data science

## 1. Introduction

Over the last decade, people have been subjected to an increasing number of natural catastrophes worldwide [1,2]. World had frequently witnessed the flooding in different

forms [3,4]. Flooding is considered the greatest calamity [5] because of its impact on life, livelihood, and resources (agricultural, livestock, and infrastructure) [6]. Floods are also the most costly natural catastrophe, accounting for 31% of all economic damage caused by disasters [7]. The number of individuals affected by floods was predicted to be at 100 million between 1995 and 2015, with an annual loss of US \$75 billion [8,9].

Bangladesh is often recognized as the most climate-vulnerable country in the world, because of its substantial low-lying land area [10–12]. Bangladesh is also regarded as the most flood-prone country because of its geographical location (i.e., unique geography, flat topography, shallow riverbed, excess rainfall) [13]. With 230 major rivers and their branches, the Ganges Delta (the world's largest river delta) alone exacerbates the issue [14,15]. Every year, it is predicted that 20–25 percent of the country is vulnerable to flooding, and this number can reach 70 percent when major flood events occur [16–18]. On average, 57.01 percent of homes were affected by various floods from 2009 to 2014, with an economic loss of US \$0.85 billion [19]. Excessive rains triggered disastrous flood events in 2017, affecting six million people, killing 134 people, and inundating over 30 percent of the country [20].

We cannot avoid the flooding because it is a natural phenomenon. However, its impact may be lessened by adopting adequate planning and management strategies [21]. It is vital to identify probable flood zones to reduce deaths and damage [22,23]. Flood susceptibility mapping is a valuable approach for identifying potential flood susceptible zones to mitigate the flooding scenarios [24,25]. Decision-makers and relevant authorities can use susceptibility mapping to design catastrophe loss mitigation strategies and policies [26]. Several flood conditioning factors can affect a flood's outburst, including topography, land use, climate, geology, and hydrological parameters. We must consider all of which when developing flood susceptibility maps. As a result, this method is known as a multi-criteria decision-making (MCDM) strategy, and it is beneficial in analyzing complicated decision processes with many criteria [27]. Several flood susceptibility models have been successfully developed and applied worldwide [28–30].

The development of remote sensing (RS) and geographic information systems (GIS) have resulted in tremendous progress in hydrological research, notably flood management and forecasting [31,32]. Flood conditioning factors can be diverse [33,34] and vary depending on geographical region [35–39]. A variety of techniques have been successfully developed and applied to produce not only flood susceptibility maps but also other natural and environmental hazards [35,37], including (a) an expert knowledge-based model (i.e., AHP [40], analytical network process (ANP) [41–44], weighted linear composite (WLC) [45]); (b) machine learning models (i.e., RF [46], artificial neural network (ANN) [47], decision tree (DT) [48], support vector machine (SVM) [49]); bagging [28] and many more (c) statistical models (i.e., frequency ratio [50,51], logistic regression [52], Shannon's entropy [53], fuzzy logic [54,55]); (d) deep learning technique, such as convolution neural network [56,57].

Past comparable studies devoted little attention to sensitivity analysis of the conditioning variables. We performed sensitivity analysis after producing the FS model with AHP. We identified the most significant conditioning variables using RF based sensitivity technique to enhance the accuracy of the FS model. Previous studies, such as soil erosion estimation [58,59], landslide susceptibility [60–62], and soil properties estimation [63,64] employed such approach. We excluded less-essential factors after performing sensitivity analysis for future modeling since they have no substantial impact on the model. As a result, based on this line of thought, we used the AHP approach to model FS again, this time with only the most significant characteristics. As a result, the new model may be more resilient than the prior model. The model's performance was evaluated using the ROC curve. For validation, only a few researchers have used both empirical and binormal ROC curves. Therefore, the outcome of the present study will help in mitigating the future floods through long-term water resource management.

The current study offered a novel effort to develop a robust FS model with fewer parameters. On the other hand, little study has been conducted in Bangladesh's northern

region. Every year, devastating floods hit this part of Bangladesh. Based on the identified research gaps and the uniqueness of the undertaking, this study aimed to generate a new FS model using the most sensitive parameters and a multi-criteria decision-making approach.

## 2. Materials and Methods

### 2.1. Materials

Since the research region is prone to frequent flooding, it is very easy to create the flood inventory using historical flood information, field survey, and Google Earth Imagery. We acquired many data types for flood susceptibility modeling in this investigation. We obtained and used Landsat-8 OLI (Operational Land Imager) to construct LULC map from the United States Geological Survey website (<https://earthexplorer.usgs.gov/>, accessed on 10 February 2022). The topographical and hydrological variables were derived from ASTER GDEM (Version 2). The Bangladesh Meteorological Department provided the rainfall data. We utilized general soil type data from the Geology Survey of Bangladesh and prepared vector map. Then, we transformed vector map into raster map in ArcGIS 10.5 software. We maintained the spatial resolution for all parameters uniformly (spatial resolution: 30 m).

### 2.2. Study Area

The north-western region (i.e., Rajshahi and Rangpur division), known as the North Bengal part of Bangladesh, is the area of focus of this study (Figure 1). The study area lies west of the Jamuna and Brahmaputra Rivers and north of the Padma River. The study area observes average annual precipitation of 250 mm. Moreover, the elevation level of the north-western region is quite flat, and the adjacent areas of the river have lower elevation. Furthermore, the slope varies from 0–47° as well as the flood-prone zones have two types of soil, including clay and a mixed form (silt, loam and clay). Again, the water level of the Brahmaputra generally starts to increase from mid-April to early May, and the water level touches its dangerous level between July–August. In contrast, between mid-May and early June, the water of the Ganges begins to rise and reaches its peak level between August and September. Moreover, the Teesta River basin is also located on the southern side of Lalmonirhat and Kurigram districts. That is why the north-western region faces river floods during the monsoon (July–October) every year because of the presence of two mighty rivers, such as the Padma and Brahmaputra. North-western region faced devastating flood events in 1988, 1998, 2004, and 2007.

### 2.3. Flood Inventory

The FS zone has been projected through the interactions between flood inventory and conditioning variables. Hence, the first stage in developing the FS map was to create the inventory [65]. However, we employed historical inundation maps, topography maps, and a survey of local people's perceptions to collect previous typical flood locations in the current research region. From the research region, we gathered 200 flood points (Figure 1b).

The flood inventory is not required for building an FS model with AHP because it is a heuristic approach and computed based on expert judgment and pair matrix [27]. This inventory data, on the other hand, were used to validate the generated flood susceptibility map.

### 2.4. Methods for Creating Flood Conditioning Parameters

The FS model is typically highly complicated and thorough because it needs numerous topographical and hydrological parameters in a spatial format. Varying magnitude of flood relies on the intensity and duration of rainfall. Various variables influence flood susceptibility, including meteorological conditions and catchment features, such as terrain, vegetation, and soil properties. In the present study, nine flood conditioning factors, combined with the catchment's geo-environmental parameters and previous literature, were initially considered to determine flood susceptibility [27,65–68]. Elevation, curvature, Topographic Position Index (TPI), slope, LULC, drainage density, Dr, soil type, and rainfall

were the variables. We used a resampling approach to make the obtained parameters consistent because they had varying spatial resolution (30 m spatial resolution). The description of the flood conditioning parameters is presented in the following section.

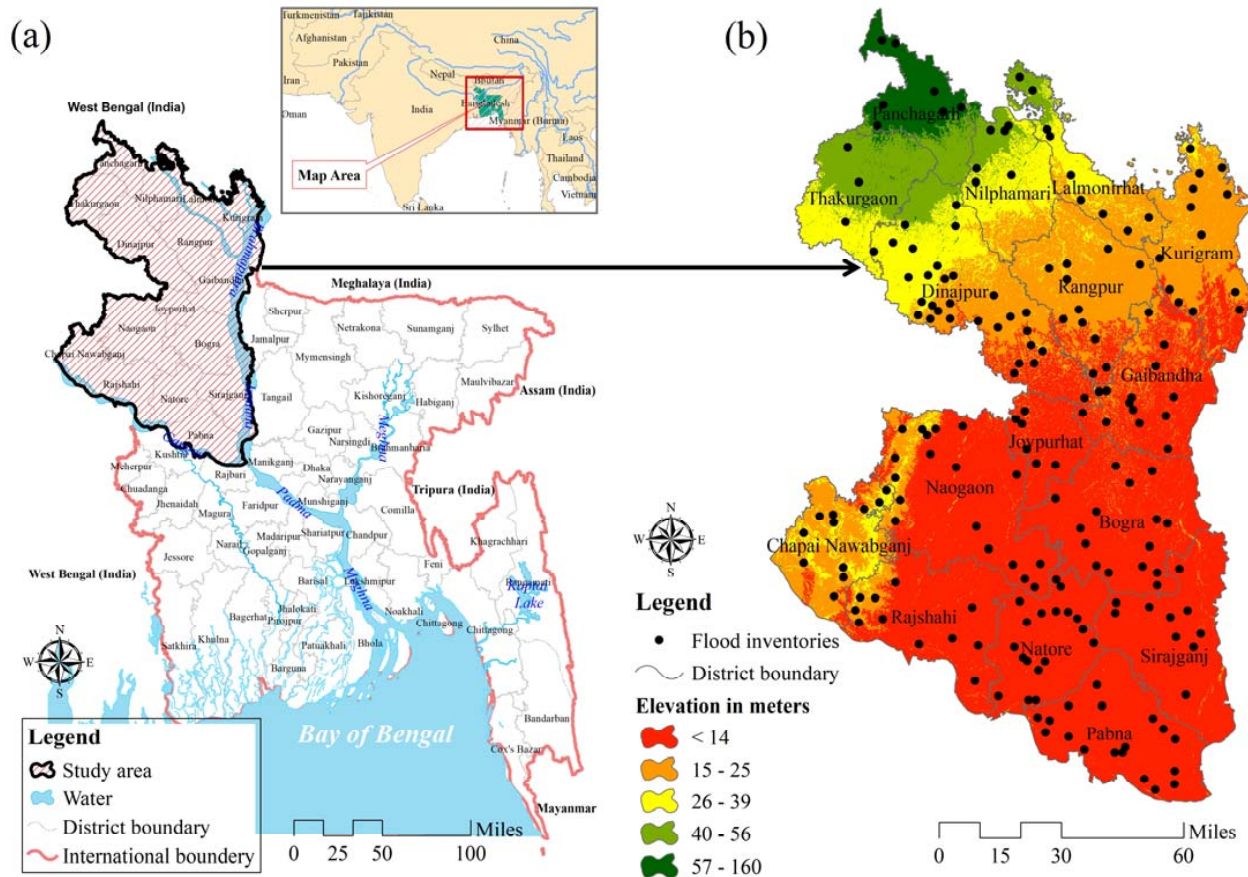


**Figure 1.** (a) Location of the study area and (b) elevation with flood inventories.

#### 2.4.1. Descriptions of Topographical Factors

Elevation is a physical factor that significantly influence the depth of the water level and control the overflow water direction [69,70]. The frequency of flooding and elevation have an inverse relationship, i.e., while elevation is lower, the probability of occurrence of flooding is higher, as the area which has high elevation is considered less susceptible to flooding [71,72]. The elevation map of this study was classified into 5 sub-groups shown in Figure 1b. The elevation map indicated that the north-western side (Panchagarh, Thakurgaon, Nilphamari) is located in a high-elevation area. That is why the susceptibility of flooding is lower, while the Southern and Eastern sides are located alongside the Brahmaputra, Jamuna, and Ganges Rivers have low susceptibility due to lower elevation. Consequently, those areas face flooding every year.

The slope angle is an important physiographic element in flood susceptibility mapping [73]. The slope angle increases the chances of flooding significantly by determining the amount of surface runoff, water flow velocity, soil erosion, and also the vertical percolation rate [74,75]. The probability of flooding depends on the slope angle as lower slope areas are more susceptible than steeper areas [76,77]. Consequently, higher importance value for computing judgment matrix can be assigned to lower slopes and vice-versa. We computed slope map from DEM with natural break algorithm based five classes: 0–0.37, 0.38–1.70, 1.17–3.30, 3.31–7.70, and 7.71–47. As found by the results, majority of the area (51%) has the lowest slope angle, and the southern part of the study area (i.e., Rajshahi, Pabna, Sirajganj, Naogaon, Kurigram) is more susceptible than the northern part because of its lower slope (0–0.37).

Curvature is the single directional rate of change in slope and is an important factor in determining potential flood zones [78]. Curvature determines convergent and divergent runoff areas, which are important in detecting flood-prone areas. Areas with negative curvatures aid runoff retention, whereas those with positive curvatures account for increased runoff [79]. Hence, comparatively higher importance value for computing judgment matrix can be assigned to the negative curvatures and vice-versa. We derived the curvature map from the DEM (Figure 2). Majority area (approx. 67%) is having mild negative to flat curvature ( $-0.01$  to  $0.2$ ), meaning that the potential for retaining runoff is comparatively higher in those regions.

Drainage density is the spacing between the channels. Areas with high drainage density respond rapidly to rainstorms, resulting in increased potential of flooding [29,80–82]. Consequently, higher importance value for computing judgment matrix can be assigned to areas with higher drainage density for this study. We classified the drainage density into 5 classes (Figure 2c). The southern part of the area (i.e., Rajshahi, Naogaon, and Natore) consists of very high drainage density ( $0.75$ – $1$ ).

TPI is generally used to measure topographic slope position and to define landform classification [83]. The positive value of TPI defines the position of the central point of elevation at a higher level than the surrounding mean elevation, and the negative value refers to a lower position than the mean elevation. Areas with negative TPI values are indicative of greater flood susceptibility, and hence higher importance value for computing judgment matrix can be assigned to them. In the present study (Figure 2d), Nagaon, Natore, Rajshahi, Sirajganj, Bogra, and Pabna have negative TPI values, which indicates that flood susceptibility is higher because of their flat surfaces.

#### 2.4.2. Descriptions of Physical Geography Factors

Rainfall significantly influences the flooding. Generally, underground hydrostatic level and water pressure increase because of high intensity of rainfall [84]. That is why heavy rainfall proportionally increases the probability of flooding [85]. Furthermore, heavy rainfall generates high potential flooding occurrence while upstream plays as a source of water because of high-intensity rainfall within a short period of time [84]. Higher importance value for computing judgment matrix can be assigned to more intensive rainfall while areas experiencing scanty rainfall can be given lower importance value while measuring flood susceptibility. Figure 3a represents the annual mean precipitation map in millimeters for the study area by dividing it into five classes. Kurigram, Gaibandha, and Sirajganj have very high rainfall intensity ( $2301$ – $2500$  mm), while low rainfall occurs in Rajshahi, Rangpur, and Dinajpur ( $1500$ – $1800$  mm).

Soil is another important factor which has crucial influence on flooding events. Surface runoff and infiltration rate are dependent on the soil characteristics [86], which adversely affected the chances of flooding [87]. The present study area is composed of 4 soil textures, including (i) silt, (ii) clay, (iii) silt loam and clay, and (iv) brown/gray soil (Figure 3b). Of these soil types, clay and mixtures of silt, loam, and clay constitute around 68% of the study. Silt and mixtures of silt, loam, and clay soil types are responsible for higher flood rates and hence can be assigned comparatively higher weights.

LULC impacts the hydrological process both directly and indirectly, for instance, in terms of infiltration, sediment transportation, infiltration, etc. [88]. Flooding is more likely to occur near major waterbodies (i.e., the Major River in the study area) because it carries more runoff from the Himalayas during the monsoons. Consequently, we provided the higher weights to areas with the major river. Furthermore, vegetated areas and open surfaces put lesser constraints on infiltration; consequently, forested areas are considered as lower flood-prone zones [48]. In this research, 4 types of LULC were identified, of which 60% of the study area falls under high intensity of development, whereas forest/crop land area comprises only 15% of the area (Figure 3c).

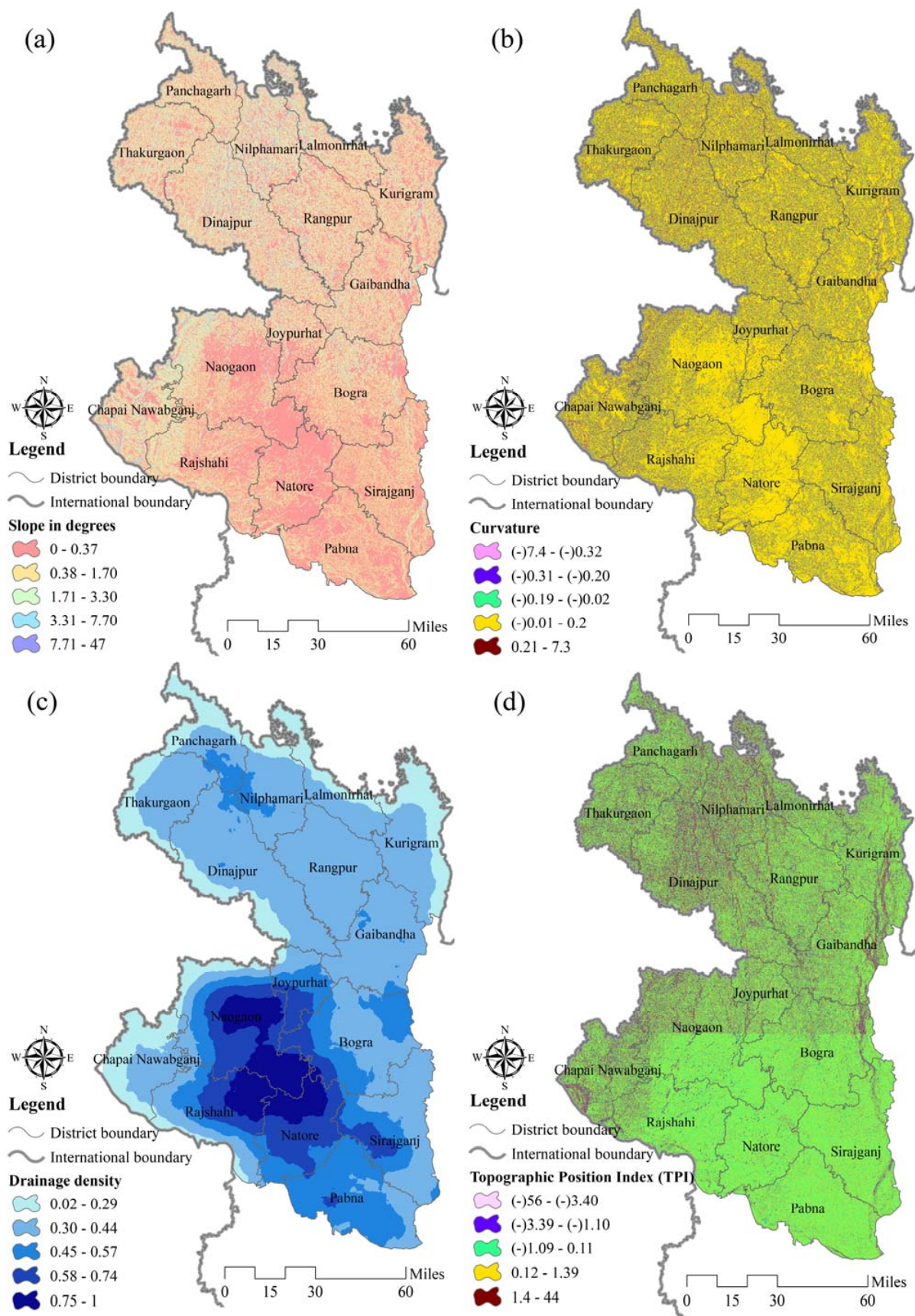
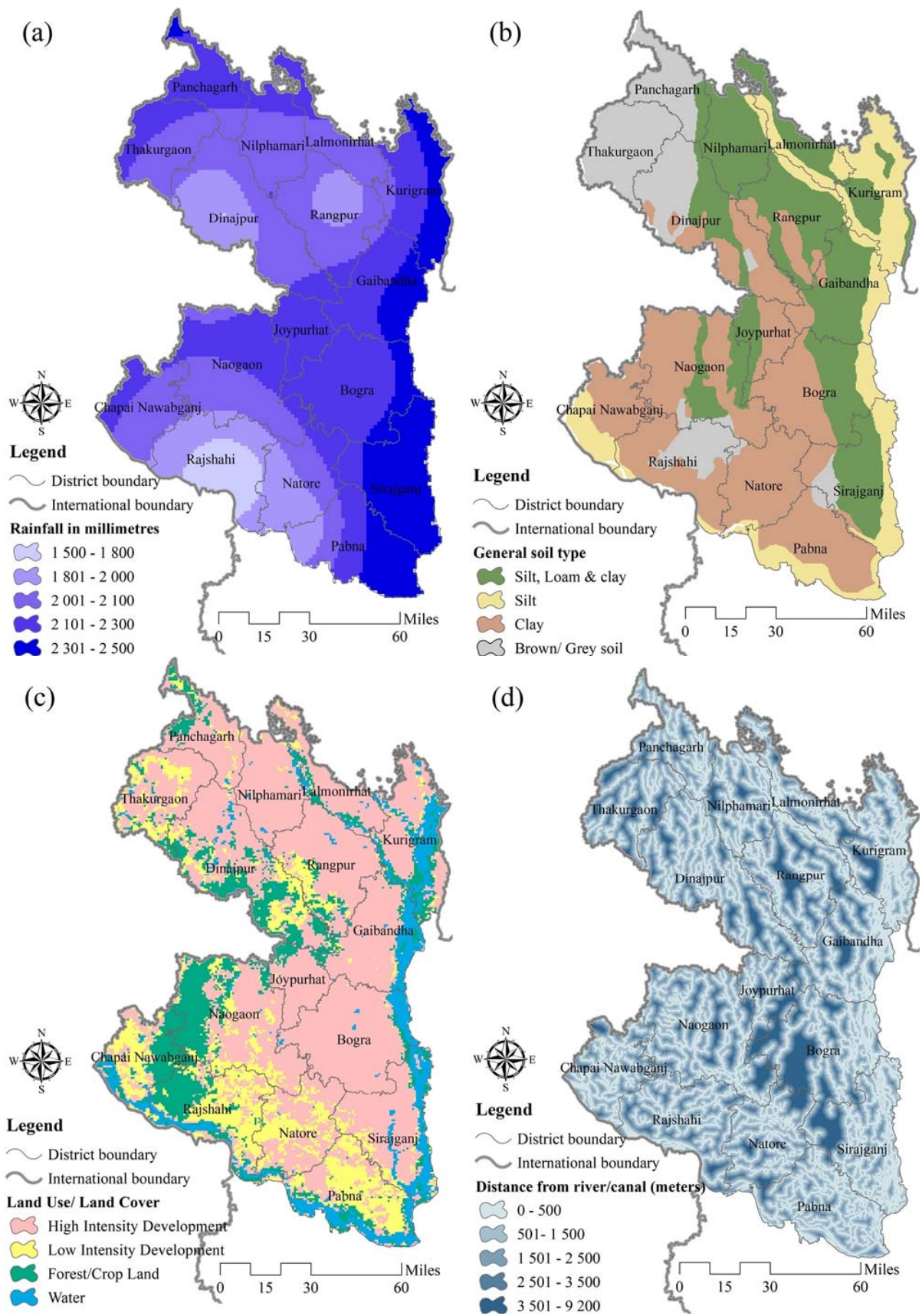


Figure 2. Spatial distribution of flood conditioning variables, such as (a) slope, (b) curvature, (c) drainage density, (d) TPI.



**Figure 3.** Spatial distribution of flood conditioning parameters, such as (a) rainfall, (b) general soil type, (c) LULC, (d) Dr.

Distance from river/canal is another important parameter relevant to flood susceptibility since the areas close to river banks are often the ones most affected by floods due to overflowing of riverbanks [89]. The probability of flooding increases while any region is close to the river/canal and decreases when the position of region is far away [90] and hence, assigned higher importance in comparison to areas close to river rivers and canals. In this article, every region of the study area is very close to the river, with about 35% of the area situated within 500 m distance from the river (Figure 3d).

### 2.5. Method for Multicolinearity Analysis

This study intends to determine if any collinear (dependent) variables were present in the dataset. The tolerance in the analysis denotes the percentage of the variation in a specific predictor that the other predictors cannot explain [61]. There is a large degree of multicollinearity when the tolerance is close to 0, and the regression coefficients' standard error will inflate. It is deemed undesirable when the variance inflation factor (VIF) exceeds around 2 [62].

### 2.6. Method for FS Modeling

Pairwise comparison matrices are the representation of factor hierarchy [91,92] and by setting the problem in this format. We computed the weights for factors and sub-factors. We determined the eigenvalues and consistency ratio (CR) using a 9-point continuous scale [93,94] weight rating. CR was calculated using Equations (1) and (2) [95,96].

$$CR = \frac{CI}{RI} \quad (1)$$

where, CI denotes the consistency index, while RI refers to the average CI

$$CI = \frac{y_{\max} - n}{(n - 1)} \quad (2)$$

where,  $y_{\max}$  = Major eigenvalue; n is the size of the comparison matrix

Saaty [97] recommended that the CR values should be less than 10 [97]. We strictly followed the instructions. Then, a GIS-based weighted overlay was performed to estimate the FS index through eigenvalues found for factors and sub-factors. Based on FS index values, we classified it into three classes using equal percentiles.

### 2.7. Method for Validation

#### 2.7.1. ROC Curves

The ROC curve is plotted with false alarm and hit rate on x and y-axis. The area under the curve (AUC) of the ROC depicts the global accuracy statistics for flood susceptible models. The prediction performance of the model rises if the AUC value (ranging from 0.5 to 1) increases [95]. There are two types of ROC curves, which have been applied in other fields, except for natural hazards, to validate the predictive models, such as parametric and non-parametric ROC curves. In the present study, we applied both ROC curves for validation.

#### 2.7.2. Other Matrices

In the present study, apart from ROC curves, the specificity, sensitivity, precision-recall curve, positive predictive value, negative predictive value, Youden index J have been used for validating the FS map.

### 2.8. Method for Sensitivity Analysis

#### 2.8.1. RF-Based Sensitivity Analysis

Breiman [96] introduced the RF algorithm, which has widely been utilized for solving the classification and regression problems. RF generates many random binary trees in order



to construct a forest. Each tree is formed using a random selection of variables taken at each node, determined by a bootstrap sample. The eventual choices on class membership and model development are based on a majority vote among all trees in the forest (output). MDA and MDG are two unique and essential measures provided by RF for ordering variables and variable selection.

### 2.8.2. Information Gain Ratio

Before practicing and validating the model, it is crucial to assess the significance of the flood susceptibility affecting parameter [98]. The Flood Influential Parameters were defined using the information gain ratio (InGR) method. In order to quantify the importance of each deciding element, its InGR significance is awarded. The greater the influence component, the higher the InGR rating. The InGR model was chosen for this study because of its consistency and efficiency, as well as the fact that it is based on Equations (3)–(6).

$$IGR(D, F) = \frac{Entropy(D) - Entropy(D, F)}{SplitEntropy(D, F)} \quad (3)$$

$$Entropy(D) = - \sum_{i=1}^2 \frac{(Y_i, F)}{|D|} \log_2 \frac{2(Y_i, F)}{|D|} \quad (4)$$

$$Entropy(D, F) = - \sum_{j=1}^m \frac{D_j}{|D|} Entropy(D) \quad (5)$$

$$SplitEntropy(D, F) = - \sum_{j=1}^m \frac{D_j}{|D|} \log_2 \frac{(D_j)}{|D|} \quad (6)$$

where  $D$  refers to the training datasets consisting of  $n$  input instances,  $n(Y_i, D)$  denotes the amount of instances in the training data  $D$  concerning with the class  $Y_i$ .

### 2.9. Method for Improving FS Model

We attempted to enhance the FS model's efficiency in this research. A series of procedures were taken in order to accomplish this. The sensitivity analysis was first carried out utilizing RF-based MDA and MGD, as well as the information gain ratio. Based on the results of three sensitivity analyses, the most and least sensitive parameters were determined in the following phases. The least sensitive parameters were then removed from the list of parameters. The weights for the selected sensitive parameters were then calculated using the AHP method. In this case, we used a sensitivity analysis-based ranking of the parameters to allocate weights to the parameters. The parameters were then incorporated in ArcGIS software's raster calculator using the calculated weights. In this manner, a new FS model was created and verified using the approaches mentioned.

## 3. Results

### 3.1. Multicollinearity Analysis

We computed the multicollinearity among the conditioning variables using TOL and VIF. The VIF and TOL should be less than 10 and 0.2 for effective FS modeling [62]. Results showed that all parameters are in range of TOL and VIF. Therefore, we can consider these variables for FS modeling. The following are the outcomes of the current study's multicollinearity analysis:

Elevation (VIF: 1.574, TOL: 0.635), slope (1.242, 0.805), curvature (1.44, 0.694), TPI (1.532, 0.653), drainage density (1.59, 0.629), distance to river (1.111, 0.9), rainfall (1.183, 0.846), soil types (1.244, 0.804), and LULC (1.245, 0.803).

### 3.2. Computation of Weights with AHP

The pairwise comparison matrices with CR and weights (eigenvalues) of the sub-criteria were computed for performing the FS model (Supplementary Table S1). Each main factor was classified into five categories except for two factors, including soil and

LULC, which were classified into four categories. All the CR values were found to be less than 0.10, which indicates ratings of the matrix were conducted randomly and preferable for flood susceptibility calculation. The factors that achieve higher eigenvalues retain an influence for flooding. The slope (0–0.37) sub-factor achieves the largest eigenvalue of 0.46, followed by curvature (−7.4 to −0.32), drainage density (0.75–1), and TPI (−3.3 to −1.1), respectively. For physical geography factors, rainfall (2301–2500), silt in general soil type, water in LULC, distance from river/canal (0–500) achieve the eigenvalues of 0.52, 0.66, 0.70, and 0.39, respectively.

Supplementary Table S2 represents the pairwise comparison matrix with other statistics computed to derive the weights of the flood conditioning variables. The calculated consistency ratio of the main factors has less than 0.10, which is acceptable. The general soil type has the highest eigenvalue at 0.22.

In the study area, the nearest area of the river where the main soil component was silt indicates the frequent flooding from the river. Rainfall has the second-highest eigenvalue (i.e., 0.20). During the monsoon period and pre-monsoon period, excessive rainfall influences flooding. The eigenvalues of Dr, LULC, and drainage density factors are 0.19, 0.15, and 0.10, respectively.

### 3.3. Flood Susceptibility Mapping and Its Validation

The flood-prone zones in the research region were identified using a GIS-based MCDA technique (i.e., AHP). In order to adequately explain and comprehend the estimated zones, the sensitive regions were categorized into three sections: (a) high, (b) moderate, and (c) low, as shown in Figure 4. Many Kurigram, Gaibandha, Bogura, Sirajganj, Pabna, Naogaon, and Chapai Nawabganj were detected as highly susceptible zones. Areas in Lalmonirhat, Nilphamry, Natore, Pabna were identified as moderate, and Thakurgaon, Panchagarh, Dinajpur, Rangpur, Joypurhat, and Rajshahi were considered as lower susceptible zones.

The high susceptibility zones have been observed in lower slope areas, which increases the likelihood of flooding. The high flood susceptibility zones have been observed along with the high drainage density areas, which contribute significantly to the likelihood of floods. The western section of the Naogaon, on the other hand, has a more extensive plant cover, which explains its location in the low susceptible zones. Kurigram and Gaibandha and Sirajganj and Pabna are located near the western banks of the Brahmaputra and Jamuna rivers; consequently, these regions have been predicted as very high susceptible zones. Similar conditions have been found in Chapai Nawabganj, Rajshahi, and Pabna, which are all located on the banks of the Padma. Similar to the Dhorla and Teesta, other rivers also influence significantly in increasing the likelihood of flooding in the Kurigram and Lalmonirhat districts. Flooding in the north-western area is also caused by the degradation of embankments and the contraction of water flow routes caused by embankments. For example, flooding in the Naogaon area occurred due to overflowing water in the Atrai and Choto-Jamuna rivers and the demolition of poor-quality embankments.

#### Validation

For the validation of the FS map, ROC curves were determined based on previous flood events data. A total of 200 random sample points were selected for validation purposes. The area under the ROC curve indicates the accuracy of the results of the maps. According to Figure 5a, the estimated susceptibility map has a higher AUC of 0.853 and 0.842 as per the empirical and binormal ROC curves, which indicates the higher accuracy of the assessment.

In addition, the Precision-recall curve (PRC) was applied to explore the accuracy of the FS model (Figure 5b). It showed that the AUC of the PRC curve is 0.869, which suggests the higher accuracy of the model.

On the other hand, we used several matrices for validating the flood susceptibility model, such as specificity (77.52), sensitivity (90.14), positive predictive value (88.72),

negative predictive value (80.04), Youden index J (0.676). These findings showed that the generated FS model has had higher accuracy and can be used for management strategies.

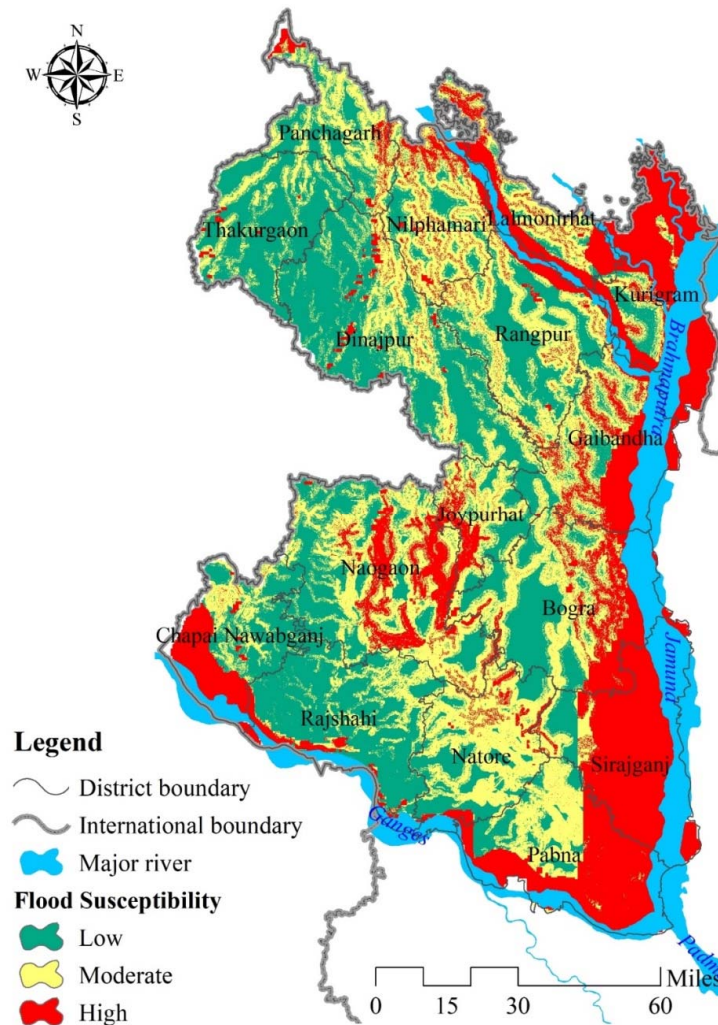


Figure 4. Spatial distribution of flood susceptibility zones.

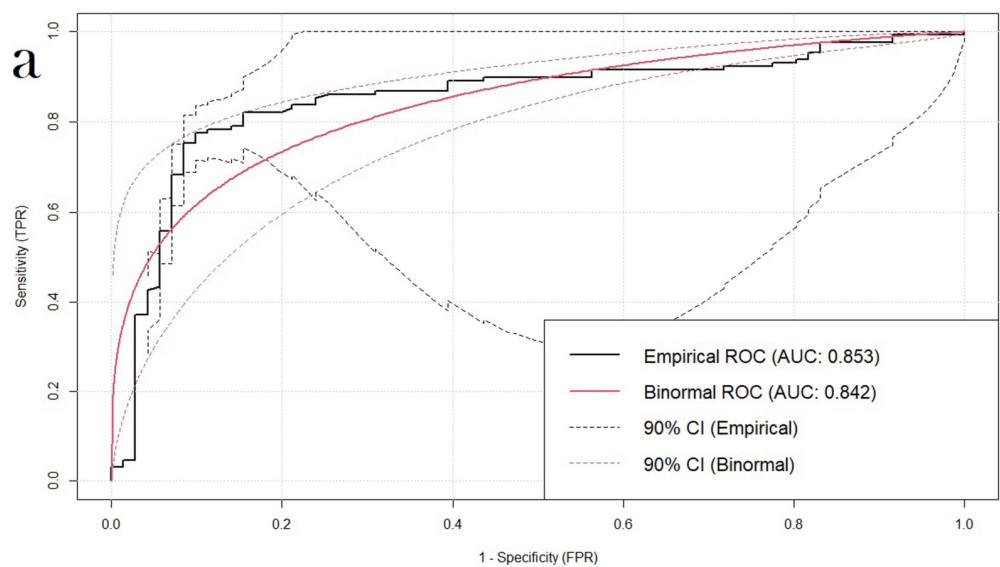
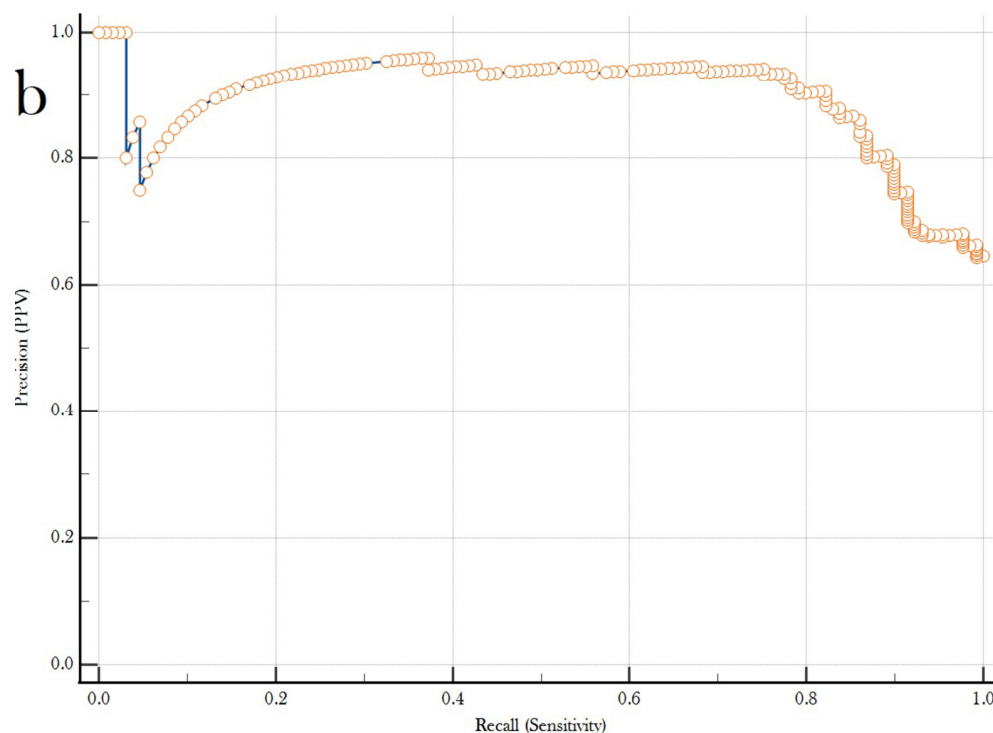


Figure 5. Cont.



**Figure 5.** Validation of the FS model using (a) ROC curves, and (b) PRC curve.

### 3.4. Sensitivity Analysis

The use of MCDA in developing an FS model indicates the probable areas with flooding using the problematic mathematical interaction between the triggering elements. However, none of the models identify any components that contribute to flooding in a given region. If we cannot identify the most influential parameters of flooding, how can we create and implement management measures to mitigate the flooding hazards.

Therefore, influential parameters identification is highly important for minimizing the damageability of the flood. As a result, determining the influential factors is critical. MDG and MDA have been used to quantify the importance of the conditioning variables. The results demonstrate that all elements were included in the FS modeling, with rainfall, TPI, soil types, distance to the river, LULC, slope, and elevation being the most relevant (Figure 6). Curvature and LULC were the least important parameters for flooding.

The information gain ratio, on the other hand, has been utilized to calculate the critical parameters. It was discovered that rainfall (0.498) was the most sensitive characteristic, followed by soil types (0.236), LULC (0.21), TPI (0.16), elevation (0.104), slope (0.075), distance to the river (0.011), drainage density ( $-0.104$ ), and curvature ( $-0.1109$ ).

According to the RF-based sensitivity and information gain ratio results, drainage density and curvature are the least sensitive factors for floods.

### 3.5. Proposed Flood Susceptibility Model and Its Validation

The findings of the validation of the FS model in the current study revealed that the previous MCDA-based FS model worked exceptionally well and delivered good results. As a result, decision-makers may utilize this model to propose sustainable flood management measures. However, no FS model is perfect. Thus researchers have constantly attempted to develop the model to deliver very high quality and solid results for management plans. As a result, while developing a robust FS model in the current work, we aimed to enhance the FS model further by integrating fewer flood conditioning factors. As a result, in a data-scarce location such as the study area (Bangladesh), researchers may use fewer factors to construct the FS with more accuracy. Thus, to develop an FS model with fewer parameters, we first attempted to identify the essential parameters in the current study.

The sensitivity analysis was carried out for this purpose, and it revealed that rainfall was the most sensitive parameter, followed by soil types, LULC, TPI, elevation, slope, distance to the river, drainage density, and curvature. Based on our observations, we decided to remove drainage density and curvature from the list of factors. Then, for the remaining parameters, we used the AHP approach once more. This time, however, we examined the sensitivity analysis-based parameter ranking. As a result, we produced weights for seven parameters (Table 1).

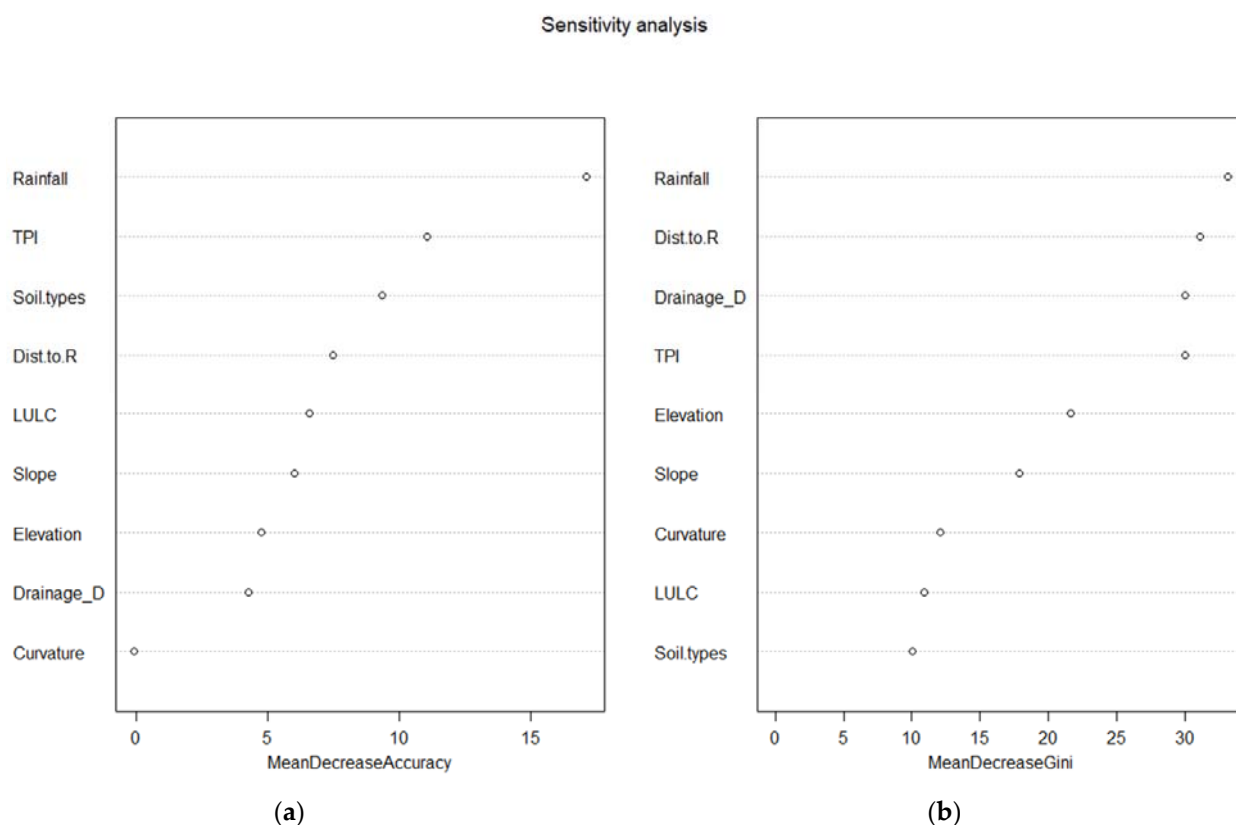


**Figure 6.** Sensitivity analysis of the FS model using RF-based (a) MDA, and (b) MDG.

**Table 1.** Pairwise comparison matrix, consistency ratio and weights of the factors for proposed flood susceptibility model.

Factors	(1)	(2)	(3)	(4)	(5)	(6)	(7)	Eigenvalues
(1) Elevation	1							0.07214
(2) Slope	1/2	1						0.049405
(3) TPI	3	4	1					0.104471
(4) Rainfall	4	5	5	1				0.283787
(5) General soil type	4	5	4	1	1			0.265354
(6) Land Use/Land Cover	3	4	4	1/2	1/2	1		0.188705
(7) Distance from river/canal	1/4	1/3	1/3	1/5	1/4	1/4	1	0.036138
Consistency Ratio CR = 0.078373								

Then, based on the calculated weights using AHP, we have integrated seven parameters in the raster calculator in ArcGIS 10.5 software. Thus, the improved flood susceptibility index (FSI) has been generated (Figure 7). The FSI has further been classified into three classes based on equal percentiles, such as high, moderate, and low FS zones. A large

portion of Kurigram, Gaibandha, Bogura, Sirajganj, Pabna, Naogaon, and Chapai Nawabganj districts have been identified as high FS zones. Moderate zones were discovered in Lalmonirhat and Natore districts. The Lower FS zones were identified in Thakurgaon, Panchagarh, Dinajpur, Rangpur, Joypurhat, and Rajshahi districts (Figure 7).

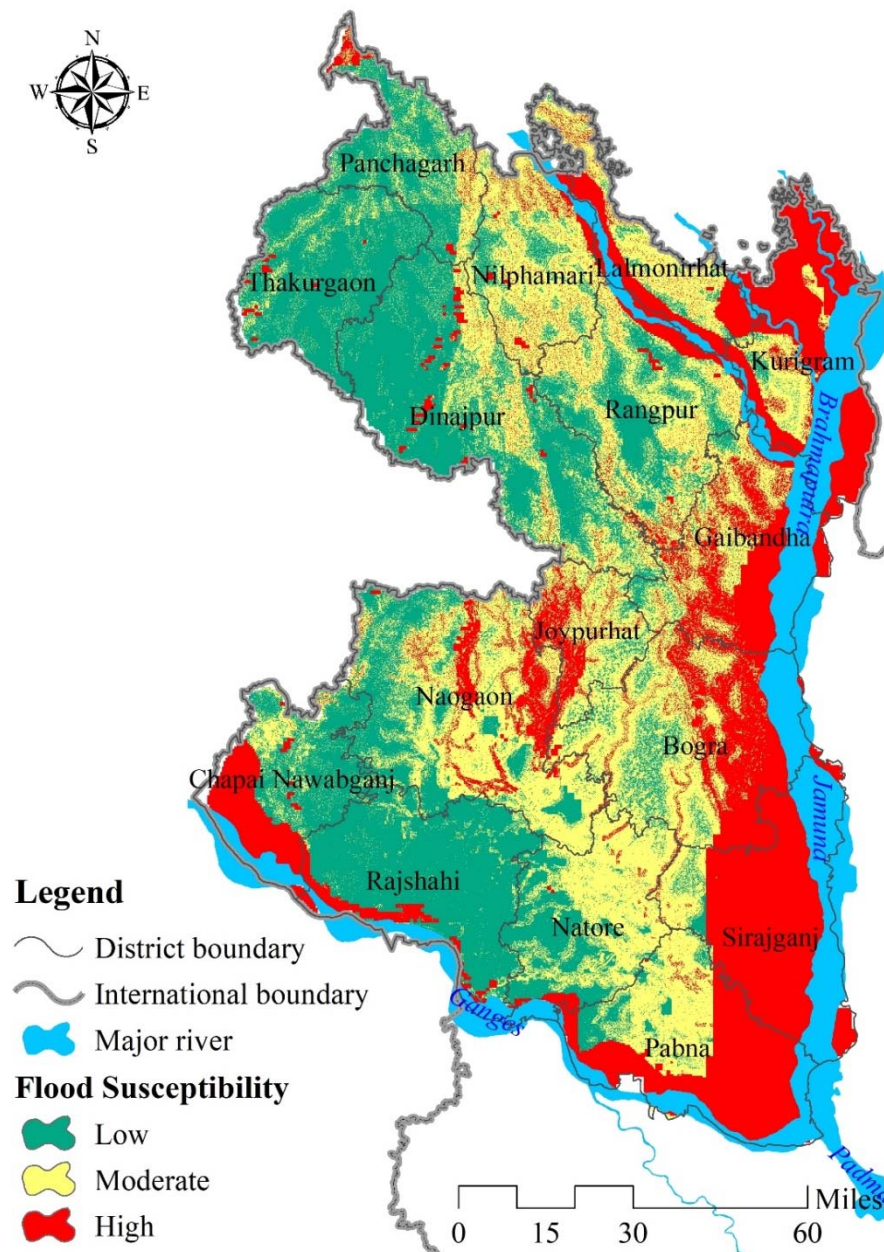


**Figure 7.** Proposed flood susceptibility model using sensitivity integrated AHP model.

#### Validation of the Proposed FS Model

Based on the total of 200 random sample points, the estimated susceptibility map has a higher AUC of 0.835 and 0.822 as per the empirical and binormal ROC curves, which indicates the higher accuracy of the assessment (Figure 8a). According to Figure 8b, the AUC of the PRC curve is 0.889, which suggests the higher accuracy of the model. For validation of the flood susceptibility model, we employed multiple matrices, including specificity (72.9), sensitivity (90.1), positive predictive value (88.043), negative predictive value (76.877), and the Youden index J. (0.6301). These data revealed that the FS model developed was more accurate and may be utilized to develop management strategies.

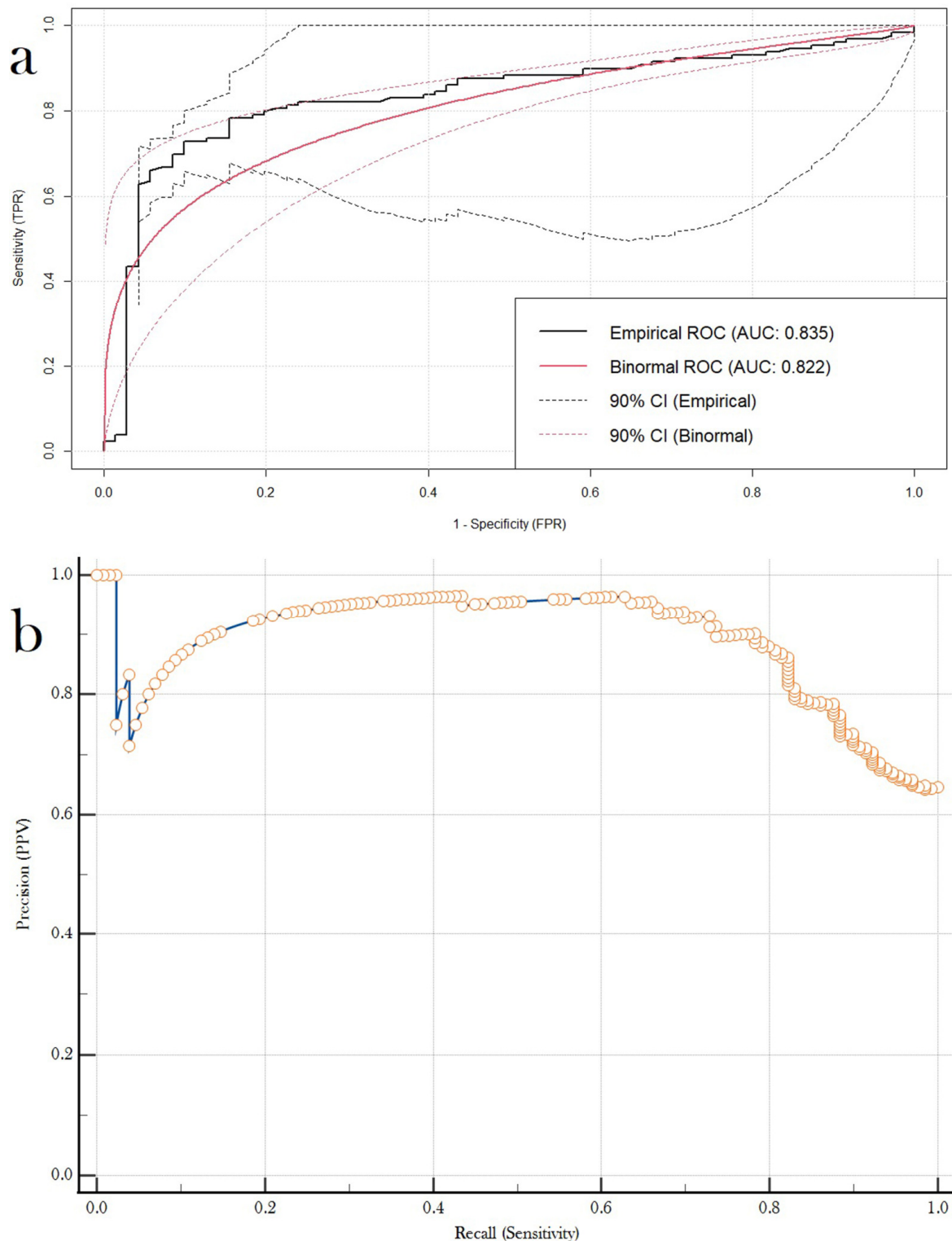


**Figure 8.** Validation of the proposed FS model using (a) ROC curves and (b) PRC curve.

The validation outcome demonstrates that the suggested FS model functioned admirably. The model exhibits a satisfactory agreement with reality according to all validation metrics. However, when compared to the prior model, it can be concluded that the suggested model differs only a little from the previous model. Given the little difference, it can be concluded that the suggested model with fewer parameters can produce a good and stable FS model. If the research area is in a data-scarce area with few datasets, this

type of work can motivate them to work with the specified key factors, which can yield extremely reliable findings and be almost equal to the FS model based on a huge number of parameters.

#### 4. Discussion

Historically, flooding has been a problem for the residents of Northwest Bangladesh, owing to heavy precipitation and overflowing rivers in the region. Thus, a proper estimate of flood susceptibility is required in order to minimize flood damage. In order to calculate flood susceptibility, a variety of data must be collected and analyzed [75,99]. Many methods for measuring flood susceptibility include logistic regression, AHP, Flood Intensity Index (IW), distance-based Pareto genetic algorithm (DBPGA), and many others. The AHP method was used to identify flood susceptibility in this study, which included nine indications. In the first model, greater factor weights were assigned to general soil type, rainfall, and Dr and LULC, with 0.22, 0.21, 0.19, and 0.15 assigned to each, respectively. To perform FS modeling with AHP, we witnessed several challenges. Many previous researchers reported that the AHP method is sometimes biased because it is subjective in nature. Expert judgment can be objective orientation. Furthermore, the machine learning algorithm can perform better than the AHP technique. However, to construct a highly accurate FS model, we first chose the important variables for modeling. FS modeling, in general, entails determining flood susceptible locations based on flood-related conditioning variables as per the characteristics of the study area [99]. Then, we assigned weights to the parameters based on their characteristics aligned with the study area and flooding event so that we could avoid bias. It is obvious that machine learning algorithms can perform better than MCDM and statistical techniques. Different approaches for FS models have been established by various researchers worldwide [99], each with its own set of drawbacks and benefits. It is important to remember that the proposed approach should be both simple and accurate. Therefore, in order to achieve robust results and somewhat close to the performance of the machine learning algorithm-based model, we employed RF (machine learning) based sensitivity analysis with field-based flooding data to investigate the most sensitive parameters. Then, we re-run the model with the most sensitive parameters to construct a robust FS model. Actually, we performed this under the circumstances of data scarcity and lack of technological know-how. Consequently, we can produce good results under these adverse circumstances. When using empirical ROC, the FS model had a higher AUC of 0.853 and a higher AUC of 0.842 when using binormal ROC, respectively. In accordance with the RF-based sensitivity and information gain ratio, the most sensitive components were rainfall, soil type, slope, and elevation. At the same time, curvature and drainage density were less sensitive features excluded from the model to simulate FS with just critical parameters. By employing empirical and binormal ROC curves, the suggested FS model obtains higher AUC values of 0.835 and 0.822, respectively, than the previous model. The suggested model, which has fewer parameters than the first model, changes slightly from the initial model and provides a stable financial model.

RF-based sensitivity and AHP analysis reveal that the average precipitation value is exceptionally high, selected as the most critical component in the data. Wang et al. [100] conducted a study and concluded the most crucial element influencing floods in the Poyang county in China, which is consistent with the conclusions of this research. Aside from that, various research on flood vulnerability showed that rainfall is recognized as the secondary source of flooding while also considering the long-term effects of flooding [101–103]. As previously said, silt covers most of the land and has an inferior infiltration capacity; as a result, flood vulnerability is determined to be higher in that location. Aside from that, the high-susceptible zone comprises places with a low slope angle and a high drainage density, which makes it particularly vulnerable. The LULC map and susceptibility map, on the other hand, make it very evident that places with heavy vegetation cover fall into the low susceptibility zone. Towards the end of their research, Azareh et al. [104] mentioned that various parameters, such as precipitation, soil composition, and topography,



were among the most relevant aspects of increasing flood vulnerability. According to recent research [105], soil texture, precipitation, elevation, and land use are the primary conditioning variables that increase the vulnerability to floods in Iran, consistent with the current study's findings. Many research [106–109] have concluded that rainfall, soil types, LULC, and distance from the river are the most critical flood conditioning elements. This is similar to the findings in this paper. The AHP technique demonstrated that the variables, such as slope, distance to stream, and LU/LC had the most significant impact on the incidence of floods in the study area, which is in line with prior findings [110,111]. According to the sensitivity analysis results, rainfall is found to be the most influencing factor for flood susceptibility in the study region, followed by general soil type and TPI. At the same time, drainage density is the least significant factor for flood susceptibility in the research area. For developing countries such as Bangladesh, where data are limited, this research could be helpful since it offered a novel susceptibility mapping technique based on fewer parameters that had not been utilized earlier. Nachappa et al. [112] investigated the use of MCDA and machine learning for FS modelling and found that the AHP and ANP MCDA approaches had high accuracy results of 0.859 and 0.866. However, both RF and SVM ML algorithms have accuracy above 0.87. In addition, many previous researchers reported that the AHP model can perform accurately for FS modeling, while the model can be enhanced by integrating some other techniques [27,110,111]. Therefore, it can be stated that most of research found the AHP-based FS model can perform better with AUC of  $<0.85$ , but can be increased by integrating some other techniques. In the present study, we integrated sensitivity analysis with AHP and found that model perform better with an AUC of 0.835, which was lower than the FS model without a sensitivity analysis. However, with fewer parameters, achieving the AUC of 0.83 is very challenging. However, it can be improved if we integrate with very important variables and other techniques. Although the result helps determine the likelihood of an imminent flood in a particular place, there are some limits. Starting with the obvious, various parameters contribute to flooding; however, owing to a paucity of data, only nine criteria were considered while mapping flood susceptibility in this study. Second, the LUCL computation was performed using moderate-resolution satellite images (30 m spatial resolution) that were made accessible for free. FS models could be more accurate if a higher resolution image is employed for parameters extraction [113]. Third, if some essential topographic parameters, such as the topographic wetness index [114] and terrain ruggedness index [115], are included in the modeling process, the FS model might produce more accurate results. Furthermore, highly sophisticated technologies such as laser scanning and HEC-RAS software can be used for generating highly accurate flooding inventories and validation datasets [115–119]. This would enhance the FS model building and validation process. These constraints should be taken into consideration in future studies.

Prior research, however, has only used a few methodologies for FS modelings, such as ROC curve validation and sensitivity analysis. In contrast, our study used a multi-criteria decision-making technique for FS modeling and empirical and binormal ROC curves for validation, which has only been completed in a few research studies. A machine learning-based sensitivity analysis was also used to identify the most sensitive components. Finally, excluding the least sensitive characteristics, the new FS model was built using just the sensitive parameters. However, no FS model is perfect. Thus, researchers have constantly attempted to develop the model to deliver top quality and solid results for management plans. As a result, rather than constructing a robust FS model based on many factors, we proposed generating a highly accurate FS model by including a smaller number of flood conditioning parameters. As a result, researchers may use fewer factors to construct the FS with more accuracy in a data-scarce location, such as the study area (developing nations such as Bangladesh and India).

## 5. Conclusions

Every year, the North-Western region of Bangladesh is affected by devastating flood events due to its geographical location and existing land use pattern. For this reason, the prediction of flood susceptible areas is highly required to mitigate the loss of lives and damage to the economy. Therefore, we proposed a sensitivity integrated AHP approach for FS modeling under the data scarcity situation in the present study. In the present study, we selected nine variables in accordance with the characteristics of the study area and flooding. Based on the selected parameters, we prepared an FS model with a standalone AHP technique. The results showed that the model performed satisfactorily. Then, we assumed that if we lack technological know-how to calculate different topographic indices, can we prepare a robust FS model? To do so, we performed a sensitivity analysis to derive the most sensitive parameters, which are readily available. Then, we re-run the model with significantly fewer parameters. The validation results showed that the model could perform well (AUC: 0.835) as the previous model. It can be stated that essential parameters with fewer numbers can generate good results. Therefore, researchers should pay attention to obtaining essential and readily available parameters in data-scarce regions.

The research findings can be very helpful for determining priority areas for applying mitigation measures, such as the construction of embankments. This priority identification is necessary, especially for low development or developing countries, such as Bangladesh, where the country cannot afford to take mitigation measures for all the risk zones at a time due to financial constraints. Furthermore, this study might be a helpful element for the concerned authorities to establish a flood monitoring-based policy in the master plan, the more contemporary Delta Plan. Future studies can address the issue of more detailed flood mitigation measures in this study area based on the results of this study.

**Supplementary Materials:** The following supporting information can be downloaded at: <https://www.mdpi.com/article/10.3390/su14073982/s1>, Table S1: Pairwise comparison matrix, consistency ratio and weights of the sub-factors; Table S2: Pairwise comparison matrix, consistency ratio and weights of the factors.

**Author Contributions:** S.K.S.: Conceptualization, Formal analysis, Methodology, Software, Visualization, Writing—original draft. S.B.A.: Data curation, Investigation, Writing—original draft. K.M.M.E.: Methodology, Writing—original draft. M.H.K.: Validation, Writing—original draft. S.T.: Conceptualization, Methodology, Software, Writing—original draft, Writing—review and editing. M.W.N.: Writing—review and editing. A.R.T.I.: Writing—review and editing. A.R.: Supervision, Writing—review and editing. A.M.: supervision; funding acquisition, writing—review and editing. All authors have read and agreed to the published version of the manuscript.

**Funding:** This study received no funding.

**Institutional Review Board Statement:** Not applicable.

**Informed Consent Statement:** Not applicable.

**Data Availability Statement:** The datasets used in the study are available from the corresponding author upon reasonable request.

**Conflicts of Interest:** The authors declare no conflict of interest.

## References

1. Hettiarachchi, S.; Wasko, C.; Sharma, A. Increase in flood risk resulting from climate change in a developed urban watershed—The role of storm temporal patterns. *Hydrol. Earth Syst. Sci.* **2018**, *22*, 2041–2056. [[CrossRef](#)]
2. Nam, W.H.; Hayes, M.J.; Svoboda, M.D.; Tadesse, T.; Wilhite, D.A. Drought hazard assessment in the context of climate change for South Korea. *Agric. Water Manag.* **2015**, *160*, 106–117. [[CrossRef](#)]
3. Jonkman, S.N.; Vrijling, J.K.; Vrouwenvelder, A.C.W.M. Methods for the estimation of loss of life due to floods: A literature review and a proposal for a new method. *Nat. Hazards* **2008**, *46*, 353–389. [[CrossRef](#)]
4. Guha-Sapir, D.; Hargitt, D.; Hoyois, P. *Thirty Years of Natural Disasters 1974–2003: The Numbers*; Presses Univ. de Louvain: Louvain-la-Neuve, Belgium, 2004.

5. Foudi, S.; Osés-Eraso, N.; Tamayo, I. Integrated spatial flood risk assessment: The case of Zaragoza. *Land Use Policy* **2015**, *42*, 278–292. [[CrossRef](#)]
6. Hirabayashi, Y.; Mahendran, R.; Koirala, S.; Konoshima, L.; Yamazaki, D.; Watanabe, S.; Kim, H.; Kanae, S. Global flood risk under climate change. *Nat. Clim. Chang.* **2013**, *3*, 816–821. [[CrossRef](#)]
7. Dano, U.L.; Balogun, A.L.; Matori, A.N.; Yusouf, K.W.; Abubakar, I.R.; Mohamed, M.A.S.; Aina, Y.A.; Pradhan, B. Flood susceptibility mapping using GIS-based analytic network process: A case study of Perlis, Malaysia. *Water* **2019**, *11*, 615. [[CrossRef](#)]
8. Alfieri, L.; Bisselink, B.; Dottori, F.; Naumann, G.; de Roo, A.; Salamon, P.; Wyser, K.; Feyen, L. Global projections of river flood risk in a warmer world. *Earth's Future* **2017**, *5*, 171–182. [[CrossRef](#)]
9. Mohanty, M.P.; Vittal, H.; Yadav, V.; Ghosh, S.; Rao, G.S.; Karmakar, S. A new bivariate risk classifier for flood management considering hazard and socio-economic dimensions. *J. Environ. Manag.* **2020**, *255*, 109733. [[CrossRef](#)]
10. USAID (2018) Bangladesh: Nutrition Profile. United States Agency for International Development, Washington, D.C. Available online: <https://www.usaid.gov/sites/default/files/documents/1864/Bangladesh-Nutrition-Profile-Mar2018-508.pdf> (accessed on 10 February 2022).
11. Sarkar, S.K.; Rahman, M.A.; Esraz-Ul-Zannat, M.; Islam, M.F. Simulation-based modeling of urban waterlogging in Khulna City. *J. Water Clim. Chang.* **2020**, *12*, 566–579. [[CrossRef](#)]
12. Fang, J.; Li, M.; Shi, P. *Mapping Flood Risk of the World*; Springer: Berlin/Heidelberg, Germany, 2015; pp. 69–102.
13. Rahman, M.; Ningsheng, C.; Islam, M.M.; Dewan, A.; Iqbal, J.; Washakh, R.M.A.; Shufeng, T. Flood Susceptibility Assessment in Bangladesh Using Machine Learning and Multi-criteria Decision Analysis. *Earth Syst. Environ.* **2019**, *3*, 585–601. [[CrossRef](#)]
14. Mirza, M.M.Q. Three recent extreme floods in Bangladesh: A hydro-meteorological analysis. *Nat. Hazards* **2003**, *28*, 35–64. [[CrossRef](#)]
15. Islam, A.S.; Bala, S.K.; Haque, M.A. Flood inundation map of Bangladesh using MODIS time-series images. *J. Flood Risk Manag.* **2010**, *3*, 210–222. [[CrossRef](#)]
16. Dewan, T.H. Societal impacts and vulnerability to floods in Bangladesh and Nepal. *Weather Clim. Extrem.* **2015**, *7*, 36–42. [[CrossRef](#)]
17. Monirul Qader Mirza, M. Global warming and changes in the probability of occurrence of floods in Bangladesh and implications. *Glob. Environ. Chang.* **2002**, *12*, 127–138. [[CrossRef](#)]
18. Dewan, A.M. *Floods in a Megacity: Geospatial Techniques in Assessing Hazards, Risk and Vulnerability*; Springer: New York, NY, USA, 2013; ISBN 9789400758759.
19. Adnan, M.S.G.; Dewan, A.; Zannat, K.E.; Abdullah, A.Y.M. The use of watershed geomorphic data in flash flood susceptibility zoning: A case study of the Karnaphuli and Sangu river basins of Bangladesh. *Nat. Hazards* **2019**, *99*, 425–448. [[CrossRef](#)]
20. Uddin, K.; Matin, M.A.; Meyer, F.J. Operational flood mapping using multi-temporal Sentinel-1 SAR images: A case study from Bangladesh. *Remote Sens.* **2019**, *11*, 1581. [[CrossRef](#)]
21. Abebe, Y.A.; Ghorbani, A.; Nikolic, I.; Vojinovic, Z.; Sanchez, A. Flood risk management in Sint Maarten—A coupled agent-based and flood modelling method. *J. Environ. Manag.* **2019**, *248*, 109317. [[CrossRef](#)]
22. Pyatkova, K.; Chen, A.S.; Butler, D.; Vojinović, Z.; Djordjević, S. Assessing the knock-on effects of flooding on road transportation. *J. Environ. Manag.* **2019**, *244*, 48–60. [[CrossRef](#)]
23. Sarhadi, A.; Soltani, S.; Modarres, R. Probabilistic flood inundation mapping of ungauged rivers: Linking GIS techniques and frequency analysis. *J. Hydrol.* **2012**, *458–459*, 68–86. [[CrossRef](#)]
24. Feng, C.C.; Wang, Y.C. GIScience research challenges for emergency management in Southeast Asia. *Nat. Hazards* **2011**, *59*, 597–616. [[CrossRef](#)]
25. Schober, B.; Hauer, C.; Habersack, H. A novel assessment of the role of Danube floodplains in flood hazard reduction (FEM method). *Nat. Hazards* **2014**, *75*, 33–50. [[CrossRef](#)]
26. Sahoo, S.N.; Sreeja, P. Development of Flood Inundation Maps and Quantification of Flood Risk in an Urban Catchment of Brahmaputra River. *ASCE-ASME J. Risk Uncertain. Eng. Syst. Part A Civ. Eng.* **2017**, *3*, 1–11. [[CrossRef](#)]
27. Das, S. Flood susceptibility mapping of the Western Ghat coastal belt using multi-source geospatial data and analytical hierarchy process (AHP). *Remote Sens. Appl. Soc. Environ.* **2020**, *20*, 100379. [[CrossRef](#)]
28. Talukdar, S.; Ghose, B.; Shahfahad; Salam, R.; Mahato, S.; Pham, Q.B.; Linh, N.T.T.; Costache, R.; Avand, M. Flood susceptibility modeling in Teesta River basin, Bangladesh using novel ensembles of bagging algorithms. *Stoch. Environ. Res. Risk Assess.* **2020**, *34*, 2277–2300. [[CrossRef](#)]
29. Quesada-Román, A.; Ballesteros-Cánovas, J.A.; Granados-Bolaños, S.; Birkel, C.; Stoffel, M. Improving regional flood risk assessment using flood frequency and dendrogeomorphic analyses in mountain catchments impacted by tropical cyclones. *Geomorphology* **2022**, *396*, 108000. [[CrossRef](#)]
30. Pinos, J.; Quesada-Román, A. Flood Risk-Related Research Trends in Latin America and the Caribbean. *Water* **2021**, *14*, 10. [[CrossRef](#)]
31. de Walque, B.; Degré, A.; Maignard, A.; Biolders, C.L. Artificial surfaces characteristics and sediment connectivity explain muddy flood hazard in Wallonia. *Catena* **2017**, *158*, 89–101. [[CrossRef](#)]
32. Poussin, J.K.; Botzen, W.J.W.; Aerts, J.C.J.H. Factors of influence on flood damage mitigation behaviour by households. *Environ. Sci. Policy* **2014**, *40*, 69–77. [[CrossRef](#)]

33. Kuriqi, A.; Koçileri, G.; Ardiçlioğlu, M. Potential of Meyer-Peter and Müller approach for estimation of bed-load sediment transport under different hydraulic regimes. *Model. Earth Syst. Environ.* **2020**, *6*, 129–137. [[CrossRef](#)]
34. Costache, R.; Tien Bui, D. Spatial prediction of flood potential using new ensembles of bivariate statistics and artificial intelligence: A case study at the Putna river catchment of Romania. *Sci. Total Environ.* **2019**, *691*, 1098–1118. [[CrossRef](#)]
35. Quesada-Román, A. Landslides and floods zonation using geomorphological analyses in a dynamic catchment of Costa Rica. Zonificación de deslizamientos e inundaciones usando análisis geomorfológicos en una cuenca dinámica de Costa Rica. *Rev. Cart.* **2021**, *102*, 125–138.
36. Wang, Y.; Hong, H.; Chen, W.; Li, S.; Panahi, M.; Khosravi, K.; Shirzadi, A.; Shahabi, H.; Panahi, S.; Costache, R. Flood susceptibility mapping in Dingnan County (China) using adaptive neuro-fuzzy inference system with biogeography based optimization and imperialistic competitive algorithm. *J. Environ. Manag.* **2019**, *247*, 712–729. [[CrossRef](#)] [[PubMed](#)]
37. García-Soriano, D.; Quesada-Román, A.; Zamorano-Orozco, J.J. Geomorphological hazards susceptibility in high-density urban areas: A case study of Mexico City. *J. S. Am. Earth Sci.* **2020**, *102*, 102667. [[CrossRef](#)]
38. Quesada-Román, A.; Villalobos-Portilla, E.; Campos-Durán, D. Hydrometeorological disasters in urban areas of Costa Rica, Central America. *Environ. Hazards* **2020**, *20*, 264–278. [[CrossRef](#)]
39. Quesada-Román, A.; Villalobos-Chacón, A. Flash flood impacts of Hurricane Otto and hydrometeorological risk mapping in Costa Rica. *Geogr. Tidsskr. Dan. J. Geogr.* **2020**, *120*, 142–155. [[CrossRef](#)]
40. Talukdar, S.; Naikoo, M.W.; Mallick, J.; Praveen, B.; Sharma, P.; Islam, A.R.M.T.; Pal, S.; Rahman, A. Coupling geographic information system integrated fuzzy logic-analytical hierarchy process with global and machine learning based sensitivity analysis for agricultural suitability mapping. *Agric. Syst.* **2022**, *196*, 103343. [[CrossRef](#)]
41. Khorrami, B.; Kamran, K.V.; Roostaei, S. Assessment of groundwater-level susceptibility to degradation based on analytical network process (ANP). *Int. J. Environ. Geoinform.* **2018**, *5*, 314–324. [[CrossRef](#)]
42. Choubin, B.; Rahmati, O.; Tahmasebipour, N.; Feizizadeh, B.; Pourghasemi, H.R. Application of fuzzy analytical network process model for analyzing the gully erosion susceptibility. In *Natural Hazards Gis-Based Spatial Modeling Using Data Mining Techniques*; Springer: Cham, Switzerland, 2019; pp. 105–125.
43. Chukwuma, E.C.; Okonkwo, C.C.; Ojediran, J.O.; Anizoba, D.C.; Ubah, J.I.; Nwachukwu, C.P. A GIS based flood vulnerability modelling of Anambra State using an integrated IVFRN-DEMATEL-ANP model. *Heliyon* **2021**, *7*, e08048. [[CrossRef](#)]
44. Gornami, R.; Shadfar, S. Application of the GIS in the Determination of Susceptible Areas to Gully Erosion Using the Analytic Network Process (ANP). *Watershed Manag. Res. J.* **2018**, *31*, 58–68.
45. Kouli, M.; Loupasakis, C.; Soupios, P.; Rozos, D.; Vallianatos, F. Landslide susceptibility mapping by comparing the WLC and WofE multi-criteria methods in the West Crete Island, Greece. *Environ. Earth Sci.* **2014**, *72*, 5197–5219. [[CrossRef](#)]
46. Lee, S.; Kim, J.C.; Jung, H.S.; Lee, M.J.; Lee, S. Spatial prediction of flood susceptibility using random-forest and boosted-tree models in Seoul metropolitan city, Korea. *Geomat. Nat. Hazards Risk* **2017**, *8*, 1185–1203. [[CrossRef](#)]
47. Kia, M.B.; Pirasteh, S.; Pradhan, B.; Mahmud, A.R.; Sulaiman, W.N.A.; Moradi, A. An artificial neural network model for flood simulation using GIS: Johor River Basin, Malaysia. *Environ. Earth Sci.* **2012**, *67*, 251–264. [[CrossRef](#)]
48. Tehrany, M.S.; Pradhan, B.; Jebur, M.N. Spatial prediction of flood susceptible areas using rule based decision tree (DT) and a novel ensemble bivariate and multivariate statistical models in GIS. *J. Hydrol.* **2013**, *504*, 69–79. [[CrossRef](#)]
49. Tehrany, M.S.; Pradhan, B.; Mansor, S.; Ahmad, N. Flood susceptibility assessment using GIS-based support vector machine model with different kernel types. *Catena* **2015**, *125*, 91–101. [[CrossRef](#)]
50. Pal, S.; Talukdar, S. Application of frequency ratio and logistic regression models for assessing physical wetland vulnerability in Punarbhaba river basin of Indo-Bangladesh. *Hum. Ecol. Risk Assess. Int. J.* **2018**, *24*, 1291–1311. [[CrossRef](#)]
51. Tehrany, M.S.; Pradhan, B.; Jebur, M.N. Flood susceptibility analysis and its verification using a novel ensemble support vector machine and frequency ratio method. *Stoch. Environ. Res. Risk Assess.* **2015**, *29*, 1149–1165. [[CrossRef](#)]
52. Nandi, A.; Mandal, A.; Wilson, M.; Smith, D. Flood hazard mapping in Jamaica using principal component analysis and logistic regression. *Environ. Earth Sci.* **2016**, *75*, 465. [[CrossRef](#)]
53. Haghizadeh, A.; Siahkamari, S.; Haghiabi, A.H.; Rahmati, O. Forecasting flood-prone areas using Shannon's entropy model. *J. Earth Syst. Sci.* **2017**, *126*, 39. [[CrossRef](#)]
54. Talukdar, S.; Mallick, J.; Sarkar, S.K.; Roy, S.K.; Islam, A.R.M.; Praveen, B.; Naikoo, M.W.; Rahman, A.; Sobnam, M. Novel hybrid models to enhance the efficiency of groundwater potentiality model. *Appl. Water Sci.* **2022**, *12*, 62. [[CrossRef](#)]
55. Alqadhi, S.; Mallick, J.; Talukdar, S.; Bindajam, A.A.; Van Hong, N.; Saha, T.K. Selecting optimal conditioning parameters for landslide susceptibility: An experimental research on Aqabat Al-Sulbat, Saudi Arabia. *Environ. Sci. Pollut. Res.* **2022**, *29*, 3743–3762. [[CrossRef](#)]
56. Yoon, J.; Gong, E.; Chatnuntawech, I.; Bilgic, B.; Lee, J.; Jung, W.; Ko, J.; Jung, H.; Setsompop, K.; Zaharchuk, G.; et al. Quantitative susceptibility mapping using deep neural network: QSMnet. *Neuroimage* **2018**, *179*, 199–206. [[CrossRef](#)] [[PubMed](#)]
57. Van Dao, D.; Jaafari, A.; Bayat, M.; Mafi-Gholami, D.; Qi, C.; Moayed, H.; Van Phong, T.; Ly, H.B.; Le, T.T.; Trinh, P.T.; et al. A spatially explicit deep learning neural network model for the prediction of landslide susceptibility. *Catena* **2020**, *188*, 104451.
58. Abdulkadir, T.S.; Muhammad, R.U.M.; Wan Yusof, K.; Ahmad, M.H.; Aremu, S.A.; Gohari, A.; Abdurrasheed, A.S. Quantitative analysis of soil erosion causative factors for susceptibility assessment in a complex watershed. *Cogent Eng.* **2019**, *6*, 1594506. [[CrossRef](#)]

59. Arabameri, A.; Yamani, M.; Pradhan, B.; Melesse, A.; Shirani, K.; Tien Bui, D. Novel ensembles of COPRAS multi-criteria decision-making with logistic regression, boosted regression tree, and random forest for spatial prediction of gully erosion susceptibility. *Sci. Total Environ.* **2019**, *688*, 903–916. [[CrossRef](#)] [[PubMed](#)]
60. Chen, W.; Zhang, S.; Li, R.; Shahabi, H. Performance evaluation of the GIS-based data mining techniques of best-first decision tree, random forest, and naïve Bayes tree for landslide susceptibility modeling. *Sci. Total Environ.* **2018**, *644*, 1006–1018. [[CrossRef](#)]
61. Mind'je, R.; Li, L.; Nsengiyumva, J.B.; Mupenzi, C.; Nyesheja, E.M.; Kayumba, P.M.; Gasirabo, A.; Hakorimana, E. Landslide susceptibility and influencing factors analysis in Rwanda. *Environ. Dev. Sustain.* **2020**, *22*, 7985–8012. [[CrossRef](#)]
62. Quesada-Román, A. Landslide risk index map at the municipal scale for Costa Rica. *Int. J. Disaster Risk Reduct.* **2021**, *56*, 102144. [[CrossRef](#)]
63. Li, M.; Zhang, L.; Liu, G. Estimation of thermal properties of soil and backfilling material from thermal response tests (TRTs) for exploiting shallow geothermal energy: Sensitivity, identifiability, and uncertainty. *Renew. Energy* **2019**, *132*, 1263–1270. [[CrossRef](#)]
64. Forkuor, G.; Hounkpatin, O.K.L.; Welp, G.; Thiel, M. High resolution mapping of soil properties using Remote Sensing variables in south-western Burkina Faso: A comparison of machine learning and multiple linear regression models. *PLoS ONE* **2017**, *12*, e0170478. [[CrossRef](#)]
65. Islam, A.R.M.T.; Talukdar, S.; Mahato, S.; Kundu, S.; Eibek, K.U.; Pham, Q.B.; Kuriqi, A.; Linh, N.T.T. Flood susceptibility modelling using advanced ensemble machine learning models. *Geosci. Front.* **2021**, *12*, 101075. [[CrossRef](#)]
66. Talukdar, S.; Eibek, K.U.; Akhter, S.; Ziaul, S.; Towfiqul Islam, A.R.M.; Mallick, J. Modeling fragmentation probability of land-use and land-cover using the bagging, random forest and random subspace in the Teesta River Basin, Bangladesh. *Ecol. Indic.* **2021**, *126*, 107612. [[CrossRef](#)]
67. Mahato, S.; Pal, S.; Talukdar, S.; Saha, T.K.; Mandal, P. Field based index of flood vulnerability (IFV): A new validation technique for flood susceptible models. *Geosci. Front.* **2021**, *12*, 101175. [[CrossRef](#)]
68. Saha, T.K.; Pal, S.; Talukdar, S.; Debanshi, S.; Khatun, R.; Singha, P.; Mandal, I. How far spatial resolution affects the ensemble machine learning based flood susceptibility prediction in data sparse region. *J. Environ. Manag.* **2021**, *297*, 113344. [[CrossRef](#)] [[PubMed](#)]
69. Choubin, B.; Moradi, E.; Golshan, M.; Adamowski, J.; Sajedi-Hosseini, F.; Mosavi, A. An ensemble prediction of flood susceptibility using multivariate discriminant analysis, classification and regression trees, and support vector machines. *Sci. Total Environ.* **2019**, *651*, 2087–2096. [[CrossRef](#)]
70. Tien Bui, D.; Pradhan, B.; Nampak, H.; Bui, Q.T.; Tran, Q.A.; Nguyen, Q.P. Hybrid artificial intelligence approach based on neural fuzzy inference model and metaheuristic optimization for flood susceptibility modeling in a high-frequency tropical cyclone area using GIS. *J. Hydrol.* **2016**, *540*, 317–330. [[CrossRef](#)]
71. Li, K.; Wu, S.; Dai, E.; Xu, Z. Flood loss analysis and quantitative risk assessment in China. *Nat. Hazards* **2012**, *63*, 737–760. [[CrossRef](#)]
72. Das, S.; Pardeshi, S.D. Morphometric analysis of Vaitarna and Ulhas river basins, Maharashtra, India: Using geospatial techniques. *Appl. Water Sci.* **2018**, *8*, 158. [[CrossRef](#)]
73. Zaharia, L.; Costache, R.; Prăvălie, R.; Minea, G. Assessment and mapping of flood potential in the Slănic catchment in Romania. *J. Earth Syst. Sci.* **2015**, *124*, 1311–1324. [[CrossRef](#)]
74. Costache, R.; Prăvălie, R.; Mitof, I.; Popescu, C. Flood vulnerability assessment in the low sector of sârăţel catchment. Case study: Joseni village. *Carpathian J. Earth Environ. Sci.* **2015**, *10*, 161–169.
75. Vojtek, M.; Vojteková, J. Flood susceptibility mapping on a national scale in Slovakia using the analytical hierarchy process. *Water* **2019**, *11*, 364. [[CrossRef](#)]
76. Kaur, H.; Gupta, S.; Parkash, S.; Thapa, R.; Mandal, R. Geospatial modelling of flood susceptibility pattern in a subtropical area of West Bengal, India. *Environ. Earth Sci.* **2017**, *76*, 339. [[CrossRef](#)]
77. Khosravi, K.; Nohani, E.; Maroufinia, E.; Pourghasemi, H.R. A GIS-based flood susceptibility assessment and its mapping in Iran: A comparison between frequency ratio and weights-of-evidence bivariate statistical models with multi-criteria decision-making technique. *Nat. Hazards* **2016**, *83*, 947–987. [[CrossRef](#)]
78. Das, S. Geographic information system and AHP-based flood hazard zonation of Vaitarna basin, Maharashtra, India. *Arab. J. Geosci.* **2018**, *11*, 576. [[CrossRef](#)]
79. Gray, D. Effect of Slope Shape on Soil Erosion. *J. Civ. Environ. Eng.* **2016**, *6*, 1000231. [[CrossRef](#)]
80. Elmore, A.J.; Julian, J.P.; Guinn, S.M.; Fitzpatrick, M.C. Potential Stream Density in Mid-Atlantic U.S. Watersheds. *PLoS ONE* **2013**, *8*, e74819. [[CrossRef](#)]
81. Pallard, B.; Castellarin, A.; Montanari, A. A look at the links between drainage density and flood statistics. *Hydrol. Earth Syst. Sci. Discuss.* **2008**, *5*, 2899–2926. [[CrossRef](#)]
82. Horton, R.E. Drainage-basin characteristics. *Eos Trans. Am. Geophys. Union* **1932**, *13*, 350–361. [[CrossRef](#)]
83. De Reu, J.; Bourgeois, J.; Bats, M.; Zwertvaegher, A.; Gelorini, V.; De Smedt, P.; Chu, W.; Antrop, M.; De Maeyer, P.; Finke, P.; et al. Application of the topographic position index to heterogeneous landscapes. *Geomorphology* **2013**, *186*, 39–49. [[CrossRef](#)]
84. Cao, C.; Xu, P.; Wang, Y.; Chen, J.; Zheng, L.; Niu, C. Flash flood hazard susceptibility mapping using frequency ratio and statistical index methods in coalmine subsidence areas. *Sustainability* **2016**, *8*, 948. [[CrossRef](#)]
85. Kay, A.L.; Jones, R.G.; Reynard, N.S. RCM rainfall for UK flood frequency estimation. II. Climate change results. *J. Hydrol.* **2006**, *318*, 163–172. [[CrossRef](#)]

86. Costache, R.; Hong, H.; Wang, Y. Identification of torrential valleys using GIS and a novel hybrid integration of artificial intelligence, machine learning and bivariate statistics. *Catena* **2019**, *183*, 104179. [[CrossRef](#)]
87. Phillips, T.H.; Baker, M.E.; Lautar, K.; Yesilonis, I.; Pavao-Zuckerman, M.A. The capacity of urban forest patches to infiltrate stormwater is influenced by soil physical properties and soil moisture. *J. Environ. Manag.* **2019**, *246*, 11–18. [[CrossRef](#)] [[PubMed](#)]
88. Zhang, X.; Cao, W.; Guo, Q.; Wu, S. Effects of landuse change on surface runoff and sediment yield at different watershed scales on the Loess Plateau. *Int. J. Sediment Res.* **2010**, *25*, 283–293. [[CrossRef](#)]
89. Chapi, K.; Singh, V.P.; Shirzadi, A.; Shahabi, H.; Bui, D.T.; Pham, B.T.; Khosravi, K. A novel hybrid artificial intelligence approach for flood susceptibility assessment. *Environ. Model. Softw.* **2017**, *95*, 229–245. [[CrossRef](#)]
90. Talukdar, S.; Pal, S. Effects of damming on the hydrological regime of Punarbhaba river basin wetlands. *Ecol. Eng.* **2019**, *135*, 61–74. [[CrossRef](#)]
91. Poudyal, C.P.; Chang, C.; Oh, H.J.; Lee, S. Landslide susceptibility maps comparing frequency ratio and artificial neural networks: A case study from the Nepal Himalaya. *Environ. Earth Sci.* **2010**, *61*, 1049–1064. [[CrossRef](#)]
92. Feizizadeh, B.; Blaschke, T. GIS-multicriteria decision analysis for landslide susceptibility mapping: Comparing three methods for the Urmia lake basin, Iran. *Nat. Hazards* **2013**, *65*, 2105–2128. [[CrossRef](#)]
93. Lootsma, F.A. Theory and Methodology Conflict resolution via pairwise comparison of concessions. *Eur. J. Oper. Res.* **1989**, *40*, 109–116. [[CrossRef](#)]
94. Lane, E.F.; Verdini, W.A. A Consistency Test for AHP Decision Makers. *Decis. Sci.* **1989**, *20*, 575–590. [[CrossRef](#)]
95. Reis, S.; Yalcin, A.; Atasoy, M.; Nisançi, R.; Bayrak, T.; Erduran, M.; Sancar, C.; Ekercin, S. Remote sensing and GIS-based landslide susceptibility mapping using frequency ratio and analytical hierarchy methods in Rize province (NE Turkey). *Environ. Earth Sci.* **2012**, *66*, 2063–2073. [[CrossRef](#)]
96. Franek, J.; Kresta, A. Judgment Scales and Consistency Measure in AHP. *Procedia Econ. Financ.* **2014**, *12*, 164–173. [[CrossRef](#)]
97. Saaty, T.L. A scaling method for priorities in hierarchical structures. *J. Math. Psychol.* **1977**, *15*, 234–281. [[CrossRef](#)]
98. Sameen, M.I.; Pradhan, B.; Lee, S. Application of convolutional neural networks featuring Bayesian optimization for landslide susceptibility assessment. *Catena* **2020**, *186*, 104249. [[CrossRef](#)]
99. Ngo, P.T.T.; Pham, T.D.; Hoang, N.D.; Tran, D.A.; Amiri, M.; Le, T.T.; Hoa, P.V.; Van Bui, P.; Nhu, V.H.; Bui, D.T. A new hybrid equilibrium optimized SysFor based geospatial data mining for tropical storm-induced flash flood susceptible mapping. *J. Environ. Manag.* **2021**, *280*, 111858. [[CrossRef](#)] [[PubMed](#)]
100. Wang, Y.; Fang, Z.; Hong, H.; Costache, R.; Tang, X. Flood susceptibility mapping by integrating frequency ratio and index of entropy with multilayer perceptron and classification and regression tree. *J. Environ. Manag.* **2021**, *289*, 112449. [[CrossRef](#)]
101. Arabameri, A.; Rezaei, K.; Cerdà, A.; Conoscenti, C.; Kalantari, Z. A comparison of statistical methods and multi-criteria decision making to map flood hazard susceptibility in Northern Iran. *Sci. Total Environ.* **2019**, *660*, 443–458. [[CrossRef](#)]
102. Zhao, G.; Pang, B.; Xu, Z.; Yue, J.; Tu, T. Mapping flood susceptibility in mountainous areas on a national scale in China. *Sci. Total Environ.* **2018**, *615*, 1133–1142. [[CrossRef](#)]
103. Santos, P.P.; Reis, E.; Pereira, S.; Santos, M. A flood susceptibility model at the national scale based on multicriteria analysis. *Sci. Total Environ.* **2019**, *667*, 325–337. [[CrossRef](#)]
104. Azareh, A.; Rafiei Sardooi, E.; Choubin, B.; Barkhori, S.; Shahdadi, A.; Adamowski, J.; Shamshirband, S. Incorporating multi-criteria decision-making and fuzzy-value functions for flood susceptibility assessment. *Geocarto Int.* **2021**, *36*, 2345–2365. [[CrossRef](#)]
105. Santangelo, N.; Santo, A.; Di Crescenzo, G.; Foscari, G.; Liuzza, V.; Sciarrotta, S.; Scorpio, V. Flood susceptibility assessment in a highly urbanized alluvial fan: The case study of Sala Consilina (southern Italy). *Nat. Hazards Earth Syst. Sci.* **2011**, *11*, 2765–2780. [[CrossRef](#)]
106. Tehrany, M.S.; Kumar, L. The application of a Dempster–Shafer-based evidential belief function in flood susceptibility mapping and comparison with frequency ratio and logistic regression methods. *Environ. Earth Sci.* **2018**, *77*, 490. [[CrossRef](#)]
107. Brath, A.; Montanari, A.; Moretti, G. Assessing the effect on flood frequency of land use change via hydrological simulation (with uncertainty). *J. Hydrol.* **2006**, *324*, 141–153. [[CrossRef](#)]
108. Arora, A.; Pandey, M.; Siddiqui, M.A.; Hong, H.; Mishra, V.N. Spatial flood susceptibility prediction in Middle Ganga Plain: Comparison of frequency ratio and Shannon’s entropy models. *Geocarto. Int.* **2021**, *36*, 2085–2116. [[CrossRef](#)]
109. Rubinato, M.; Nichols, A.; Peng, Y.; Zhang, J.-M.; Lashford, C.; Cai, Y.-P.; Lin, P.-Z.; Tait, S. Urban and river flooding: Comparison of flood risk management approaches in the UK and China and an assessment of future knowledge needs. *Water Sci. Eng.* **2019**, *12*, 274–283. [[CrossRef](#)]
110. Zou, Q.; Zhou, J.; Zhou, C.; Song, L.; Guo, J. Comprehensive flood risk assessment based on set pair analysis-variable fuzzy sets model and fuzzy AHP. *Stoch. Environ. Res. Risk Assess.* **2013**, *27*, 525–546. [[CrossRef](#)]
111. Shafapour Tehrany, M.; Shabani, F.; Neamah Jebur, M.; Hong, H.; Chen, W.; Xie, X. GIS-based spatial prediction of flood prone areas using standalone frequency ratio, logistic regression, weight of evidence and their ensemble techniques. *Geomat. Nat. Hazards Risk* **2017**, *8*, 1538–1561. [[CrossRef](#)]
112. Nachappa, T.G.; Piralilou, S.T.; Gholamnia, K.; Ghorbanzadeh, O.; Rahmati, O.; Blaschke, T. Flood susceptibility mapping with machine learning, multi-criteria decision analysis and ensemble using Dempster Shafer Theory. *J. Hydrol.* **2020**, *590*, 125275. [[CrossRef](#)]

113. Mallick, J.; Talukdar, S.; Ahmed, M. Combining high resolution input and stacking ensemble machine learning algorithms for developing robust groundwater potentiality models in Bisha watershed, Saudi Arabia. *Appl. Water Sci.* **2022**, *12*, 12–27. [[CrossRef](#)]
114. Granados-Bolaños, S.; Quesada-Román, A.; Alvarado, G.E. Low-cost UAV applications in dynamic tropical volcanic landforms. *J. Volcanol. Geotherm. Res.* **2021**, *410*, 107143. [[CrossRef](#)]
115. Shustikova, I.; Domeneghetti, A.; Neal, J.C.; Bates, P.; Castellarin, A. Comparing 2D capabilities of HEC-RAS and LISFLOOD-FP on complex topography. *Hydrol. Sci. J.* **2019**, *64*, 1769–1782. [[CrossRef](#)]
116. Costabile, P.; Costanzo, C.; Ferraro, D.; Barca, P. Is HEC-RAS 2D accurate enough for storm-event hazard assessment? Lessons learnt from a benchmarking study based on rain-on-grid modelling. *J. Hydrol.* **2021**, *603*, 126962. [[CrossRef](#)]
117. Dazzi, S.; Shustikova, I.; Domeneghetti, A.; Castellarin, A.; Vacondio, R. Comparison of two modelling strategies for 2D large-scale flood simulations. *Environ. Model. Softw.* **2021**, *146*, 105225. [[CrossRef](#)]
118. Wing, O.E.; Bates, P.D.; Sampson, C.C.; Smith, A.M.; Johnson, K.A.; Erickson, T.A. Validation of a 30 m resolution flood hazard model of the conterminous United States. *Water Resour. Res.* **2017**, *53*, 7968–7986. [[CrossRef](#)]
119. Costabile, P.; Costanzo, C.; De Lorenzo, G.; De Santis, R.; Penna, N.; Macchione, F. Terrestrial and airborne laser scanning and 2-D modelling for 3-D flood hazard maps in urban areas: New opportunities and perspectives. *Environ. Model. Softw.* **2021**, *135*, 104889. [[CrossRef](#)]